Journal of
Mechanics of
Materials and Structures

A THREE DIMENSIONAL CONTACT MODEL FOR SOIL-PIPE INTERACTION

Nelly Piedad Rubio, Deane Roehl and Celso Romanel

A THREE DIMENSIONAL CONTACT MODEL FOR SOIL-PIPE INTERACTION

NELLY PIEDAD RUBIO, DEANE ROEHL AND CELSO ROMANEL

One of the most common causes of collapse of pipelines crossing unstable slopes is the large deformation induced by landslides. This paper presents a numerical methodology based on the finite element method for the analysis of buried pipelines considering the nonlinear behavior of the soil-pipe interface. This problem is inherently complex since it involves the interaction between two different bodies (pipe and soil), and is affected by many elements such as material nonlinearities, local and global buckling, soil settlement, pipe upheaval, among others. An important aspect that should be considered in the study of buried pipes is the mechanical behavior along the interface between the structure and the soil. The contact problem, which includes both a normal and a tangential constitutive law, is formulated through a penalty method. The finite element model considers full three-dimensional geometry, elasto-plastic material behavior and accounts for the presence of large displacements and deformations.

1. Introduction

In Brazil transport of petroleum, gas and oil derivatives between refineries and the port tanking terminals that collect and export petroleum products is generally made through buried pipelines that cross the mountain range of Serra do Mar. These mountains run parallel to the Atlantic Coast and stand between the Brazilian plateau, where most of the largest cities are located, and the lower sea plains.

A major concern during design and performance monitoring of these buried structures is the potential occurrence of soil movements, usually triggered by heavy rainfalls in areas lacking protective forest covering or those that have recently experienced changes of landscape caused by excavations, cuts and embankments due to road constructions, new industrial developments, etc. In cases of pipeline damage the consequences may be quite severe in terms of economical losses, social and environmental impacts. For example, the rupture of an expansion gasket during oil pumping in the state of Paraná in 2000 provoked a leakage of more than a million gallons of crude oil, endangering fauna and flora in addition to interrupting the distribution of potable water to the population of nearby towns.

Many analytical and computational procedures for the investigation of the mechanics of soil-pipe interaction problems are presented in the literature. The available numerical solutions are generally based on the finite element method and consider models ranging from simple one-dimensional beam models [Zhou and Murray 1993; Zhou and Murray 1996; Lim et al. 2001] and two-dimensional analysis of buried galleries [Katona 1983], to shell models [Selvadurai and Pang 1988]. Numerical models based on the boundary element model have also been employed [Mandolini et al. 2001]. Moreover, many different material models have been adopted to represent soil behavior, the most popular of which are elastic and elasto-plastic models.

In the analysis of the behavior of buried pipes one very important aspect is the consideration of the interface behavior. This problem is inherently complex since it involves the interaction between two different bodies (pipe and soil) and is affected by many elements such as material nonlinearities, local and global buckling, soil settlement, pipe upheaval, among others. Various possible modes of deformation must be taken into account, including the stick and slip modes, for which normal stress remains compressive, as well as the debonding and rebonding modes, for which normal stress can reach zero. Models for the pipe-soil interface describe limiting cases such as perfect adhesion [Selvadurai and Pang 1988], elastic and inelastic springs for both transversal and longitudinal behavior [Zhou and Murray 1993], and continuum interface elements as in the pioneer works [Katona 1983; Desai et al. 1984]. More realistic continuum contact models including both normal and longitudinal contact forces models can be generically framed as optimization models, by which the contact constraints are introduced in the general equations of motion through a Lagrangian multiplier formulation and solved through mathematical programming algorithms. A long list of authors who have adopted this strategy includes [Simo et al. 1985; Kwak and Lee 1988; Lee et al. 1994; Laursen and Simo 1993; Ferreira and Roehl 2001]. Alternatively, the contact conditions are satisfied empirically through a penalty based formulation. Examples of this type of contact model are [Bathe and Chaudhary 1985; Peric and Owen 1992; Laursen 2002].

This paper presents a numerical methodology based on the finite element method for the analysis of buried pipelines considering the nonlinear behavior of the soil-pipe interface. The finite element model considers full three-dimensional geometry, elasto-plastic material behavior and accounts for the presence of large displacements and deformations. Both pipe and soil are modeled with hexahedral enhanced assumed strain elements. The numerical solution procedure is based on an incremental, iterative procedure, forming a sequence of nonlinear incremental problems solved by a Newton–Raphson scheme. The solution of boundary problems subject to the normal contact restrictions (impenetrability and compressive normal tractions at contact) and to the friction law (tangential constitutive law) is carried out here with a penalty formulation, by which the contact restrictions are approximated through an easy-to-implement procedure. The incremental evolution equations for the contact constitutive model are obtained through numerical integration with an implicit Euler algorithm. The element stiffness and contact matrices are obtained in the framework of a consistent linearization of the contact virtual work. Finally, application of the model to a slowly sliding slope with buried pipe is presented.

2. Continuum governing equations

2.1. *Equations of motion.* The formulation of the contact problem presented in this work is based on the work of Laursen and Simo [1993] and is reviewed here for the case of two deformable bodies $\boldsymbol{B}^i$ for $i = 1, 2$ in the space $\Re^3$ as shown in Figure 1. We assume that the bodies are contact-free in the corresponding reference configurations Ω^1 and Ω^2 at time $t = 0$. The subsequent configurations indicated as ϕ_t^1, ϕ_t^2 cause the two bodies to physically come into contact introducing interactive forces. The contact surfaces are represented by $\Gamma^{(1)}$ and $\Gamma^{(2)}$, the so-called *slave* and *master* surfaces, respectively. The current surface location is given by $\gamma^{(i)} = \phi_t^i(\Gamma^{(i)})$. In the initial configuration, material points on $\Gamma^{(1)}$ and $\Gamma^{(2)}$ are represented by $\boldsymbol{X}$ and $\boldsymbol{Y}$, respectively; correspondingly, the current configuration is given by $\boldsymbol{x} = \varphi_t^{(1)}(\boldsymbol{X})$ and $\boldsymbol{y} = \varphi_t^{(2)}(\boldsymbol{Y})$.
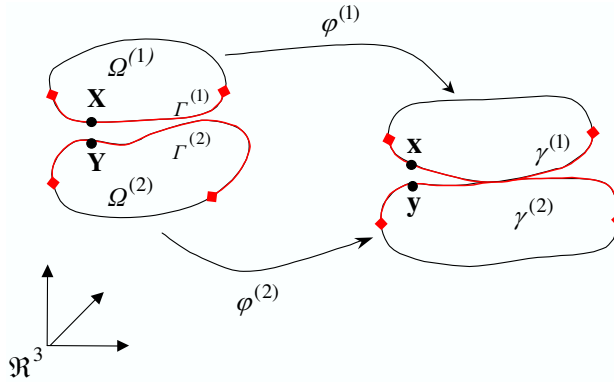
Figure 1. Body configurations at $t = 0$ and general t.

Assuming a quasistatic response and considering a description of motion in the reference configuration, the classical equations of motion for each body i at time t are given by

$$\text{DIV} P_t^{(i)} + f_t^{(i)} = 0 \quad \text{in } \mathbf{\Omega}^{(i)}, \qquad P_t^{(i)} n_0^{(i)} = \overline{t_t^{(i)}} \quad \text{in } \mathbf{\Gamma}_\sigma^{(i)}, \qquad \varphi_t^{(i)} = \overline{\varphi_t^{(i)}} \quad \text{in } \mathbf{\Gamma}_\varphi^{(i)}, \tag{1}$$

where $P_t^{(i)}$ is the first Piola–Kirchhoff stress tensor, $f_t^{(i)}$ is the prescribed body force, $n_0^{(i)}$ is the outward normal in the reference configuration, $\Gamma_\sigma^{(i)}$, $\Gamma_\phi^{(i)}$ are, respectively, the parts of $\partial\Omega^{(i)}$ where the tractions $t_t^{(i)}$ and displacements $\phi_t^{(i)}$ are given, and $P_t^{(i)}$ is assumed to be given by a hyperelastic constitutive law.

2.2. *Frictional contact formulation.* For a pair of motions $\phi^{(1)}(\cdot, t)$, $\phi^{(2)}(\cdot, t)$, the impenetrability restriction can be formulated for all points $X \in \Gamma^{(1)}$ by first identifying a potential contact point $Y_-(X, t)$ on the master surface according to the following closest point projection in the spatial configuration:

$$Y_-(X, t) = \arg \min_{Y \in \Gamma_c^{(2)}} \left\| \varphi^{(1)}(X, t) - \varphi^{(2)}(Y, t) \right\|.$$

To formulate the contact conditions, a configuration-dependent differentiable distance function is introduced, which will be constrained to guarantee physical impenetrability.

For a pair X, Y_-, a gap function may be defined as $g(X, t) = -\nu\big(\varphi^{(1)}(X, t) - \varphi^{(2)}(Y_-, t)\big)$, where ν is the outward unit normal to the $\gamma^{(2)}$ at $y = \phi_t^{(2)}(Y)$ as illustrated in Figure 2. Then, the definition of $g(X, t)$ is given in terms of the closest point projection of $x = \phi_t^i(X)$ onto the opposing surface $\gamma_c^{(2)}$. The impenetrability condition is formulated as $g(X, t) \le 0$.

Furthermore, the complementarity conditions are connected to the superficial contact force $t^{(1)}(X, t) = P^{(1)}(X, t) \cdot n_0^{(1)}(X)$, where $P^{(1)}(X, t)$ is the first Piola–Kirchhoff tensor at X and $n_0^{(1)}(X)$ is the outward normal at X in the reference configuration. This surface force may therefore be written as

$$t^{(1)}(X, t) = t_N(X, t)\nu + P_\nu t^{(1)}(X, t), \tag{2}$$

where $P_\nu t^{(1)}$ is the projection of $t^{(1)}$ onto the associated tangent plane, and $t_N(X, t)$ represents the contact pressure at X.
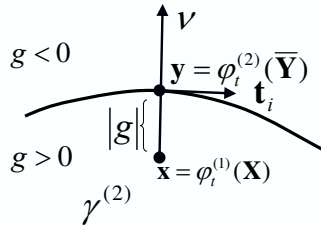
Figure 2. Contact problem and unit outward normal.

The Kuhn–Tucker conditions for normal contact are given by

$$g(X, t) \leq 0, \qquad t_N(X, t) \geq 0, \qquad t_N(X, t)g(X, t) = 0, \qquad t_N(X, t)\dot{g}(X, t) = 0. \tag{3}$$

The first three conditions reflect the impenetrability constraint, the compressive normal traction constraint, and the requirement that the pressure is nonzero only when contact takes place, that is, the gap function $g = 0$, respectively. The last requirement is the persistency condition used when considering frictional kinematics.

Once the impenetrability constraint $(3)_1$ induces a geometric structure through the gap function, an associated convective basis, adequate for definition of the frictional constraints, is necessary. Parameterizations for $\Gamma^{(i)}$ and $\gamma^{(i)}$ are adopted for body 2 (see Figure 3) according to the definition of a series of time indexed mappings $\Psi_t^{(i)} : A^{(i)} \to \Re^{n-1}$, with $\Gamma^{(i)} = \Psi_0^{(i)}(A^{(i)})$, $\gamma^{(i)} = \Psi_t^{(i)}(A^{(i)})$ and $\Psi_t^{(i)} = \varphi_t^{(i)0}\Psi_0^{(i)}$. The dimension of the contact surface $\Gamma^{(i)}$ is one dimension lower than the number of spatial dimensions involved in the kinematic description. In the three-dimensional case, one point $\xi \in A^{(2)}$ is given by $\boldsymbol{\xi} = (\xi^1, \xi^2)$. Bases for $\boldsymbol{\Gamma}^{(2)}$ and $\gamma^{(2)}$ are conveniently defined by partial derivatives with respect to these variables:

$$\boldsymbol{E}_\alpha(\boldsymbol{\xi}) = \boldsymbol{\Psi}_{0,\alpha}^{(2)}(\xi), \qquad \boldsymbol{e}_\alpha(\boldsymbol{\xi}) = \boldsymbol{\Psi}_{t,\alpha}^{(2)}(\xi) = \boldsymbol{F}_t^{(2)}\big(\boldsymbol{\Psi}_0^{(2)}(\boldsymbol{\xi})\big)\boldsymbol{E}_\alpha(\boldsymbol{\xi}), \qquad \alpha = 1, 2.$$

In the above equations $\boldsymbol{F}_t^{(2)}$ is the gradient deformation corresponding to $\varphi^{(2)}$. Subscript $,\alpha$ represents derivatives with respect to ξ^α. For any point $X \in \Gamma^{(1)}$, a point $Y \in \Gamma^{(2)}$ is assigned such that Y_- is obtained through minimization.

Correlated points y_- and ξ_- in the spatial and parametric domains, respectively, are defined as

$$\boldsymbol{Y}_0(X, t) = \boldsymbol{\psi}_0^{(2)}\big(\xi_-(X, t)\big), \qquad \boldsymbol{y}_-(X, t) = \boldsymbol{\psi}_t^{(2)}\big(\xi_-(X, t)\big).$$

Identification of ξ_- with point X depends upon the motions of both bodies. The specific basis for ξ_- is

$$T_\alpha = E_\alpha(\xi_-), \qquad t_\alpha = e_\alpha(\xi_-), \qquad \alpha = 1, 2.$$

Tangent vectors $\boldsymbol{T}_\alpha$ and $\boldsymbol{t}_\alpha$ describe a convective basis at point X relative to $\Gamma^{(2)}$. The normal vector is defined as $\boldsymbol{v} = (\boldsymbol{t}_1 \times \boldsymbol{t}_2)/\|\boldsymbol{t}_1 \times \boldsymbol{t}_2\|$.

According to the persistency condition, if $\dot{g}(X, t) = 0$, the time rate of change of the relative position vector between $\boldsymbol{x} = \phi^{(1)}$ and $y_- = \phi^{(2)}(Y_-(X, t), t)$ must be zero. The evaluation of this time derivative
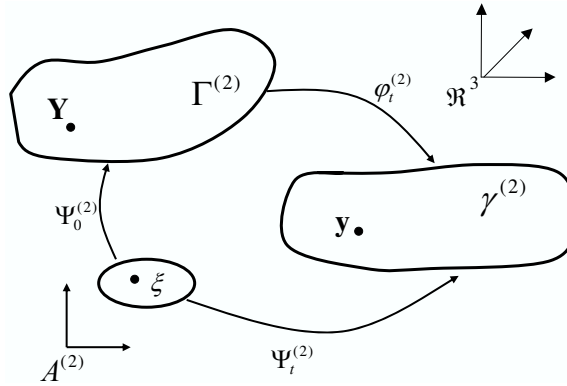
Figure 3. Parameterizations for $\Gamma^{(i)}$ and $\gamma^{(i)}$.

gives an important expression for the material relative velocity of X, namely,

$$\boldsymbol{V}^{(1)}(\boldsymbol{X},t) - \boldsymbol{V}^{(2)}\big(\boldsymbol{Y}_-(\boldsymbol{X},t),t\big) = \boldsymbol{F}_t^{(2)}\big(\boldsymbol{\Psi}_0^{(2)}(\boldsymbol{\xi}_-)\big)\frac{d}{dt}[\overline{\boldsymbol{Y}}(\boldsymbol{X},t)].$$

In the above equation, the left side gives the relative material velocities of X and Y_-, thus physically representing the slip rate of X relative to the adjacent surface $\gamma^{(2)} = \phi^{(2)}(\Gamma^{(2)})$. The right hand side of this equation represents the geometry that is used in the definition of frictional evolution law.

$$V_T(\boldsymbol{X},t) := \frac{d}{dt}[Y_-(\boldsymbol{X},t)] = \dot{\xi}^\beta_-(\boldsymbol{X},t)\boldsymbol{T}_\alpha.$$

Mathematically, $V_T(\boldsymbol{X},t)$ represents the relative tangential velocity and, by the assumption of $\dot{g}(\boldsymbol{X},t)=0$ it contains no normal component. It is convenient to express V_T in a dual basis. One can define the dual basis vector, the metrics and the inverse metrics. The spatial counterpart of the material relative velocity $V_T(\boldsymbol{X},t)$ is obtained through push forward transformation to the spatial frame. It and the frictional traction are expressed in the dual basis as

$$\boldsymbol{v}_T^b(\boldsymbol{X},t) = M_{\alpha\beta}\dot{\xi}^\beta_-(\boldsymbol{X},t)\boldsymbol{t}^\alpha, \qquad \boldsymbol{t}_T^b(\boldsymbol{X},t) := -P_v\boldsymbol{t}^{(1)}(\boldsymbol{X},t) := t_{T\alpha}(\boldsymbol{X},t)\boldsymbol{t}^\alpha.$$

Based on the description of slip velocity and traction, the Coulomb friction model is stated as

$$\boldsymbol{\Phi} := \|\boldsymbol{t}_T^b\| - \mu t_N \leq 0, \qquad \boldsymbol{v}_T^b - \zeta\frac{\boldsymbol{t}_T^b}{\|\boldsymbol{t}_T^b\|} = 0, \qquad \zeta \geq 0, \qquad \boldsymbol{\Phi}\zeta = 0, \tag{4}$$

which are the friction law, relative tangential velocity, the irreversibility of slip, and the complementarity condition. In the above formulation μ is the friction coefficient with hardening effects excluded, t_N and t_T are the normal and tangential contact forces, $\boldsymbol{v}_T$ is the relative tangential velocity. Frictional traction and velocity are expressed in dual basis, according to the large deformation theory. More details on the frictional contact formulation can be found in [Laursen and Simo 1993; Laursen 2002; Rubio et al. 2003].

2.3. *Formulation of the virtual work of contact.* We consider the approximate weak form of the global equilibrium equations. The test function $\phi^{*(i)} : \Omega(i) \to R^3$ satisfies the condition $\phi^{*(i)} = 0$ on $\Gamma_\phi^{(i)}$. Restrictions placed upon $\phi^{*(i)}$ by the contact conditions are not imposed since such limitations are to

be removed using the penalty regularization introduced above. Multiplying Equations (1) by $\phi^{*(i)}$ and integrating by parts over $\Omega^{(i)}$ we obtain the weak form of the equilibrium:

$$G^{(i)}(\varphi_t^{(i)}, \varphi^{*(i)}) := \int_{\Omega^{(i)}} P_t^{(i)} \cdot GRAD[\varphi^{*(i)}]d\Omega^{(i)} - \int_{\Omega^{(i)}} f_t^{(i)} \cdot \varphi^{*(i)}d\Omega^{(i)} - \int_{\Gamma_\sigma^{(i)}} \overline{t^{(i)}} \cdot \varphi^{*(i)}d\Gamma_\sigma^{(i)},$$

$$G^{(i)}(\varphi_t^{(i)}, \varphi^{*(i)}) := \int_{\Gamma^{(i)}} \overline{t_t^{(i)}} \cdot \varphi^{*(i)}d\Gamma^{(i)}.$$

The quantity $G^{(i)}$ is the sum of the internal virtual work and the virtual work of the applied forces and tractions for body i. The balance of the virtual work of the contact forces acting on $\Gamma^{(i)}$ is

$$G(\varphi_t, \varphi^*) := G^{(1)}(\varphi_t^{(1)}, \varphi^{*(2)}) + G^{(2)}(\varphi_t^{(2)}, \varphi^{*(2)}) = \int_{\Gamma^{(1)}} \overline{t_t^{(1)}} \cdot \varphi^{*(1)}d\Gamma^{(1)} + \int_{\Gamma^{(2)}} \overline{t_t^{(2)}} \cdot \varphi^{*(2)}d\Gamma^{(2)},$$

where ϕ_t is the collection of mappings $\phi_t^{(1)}$ and $\phi_t^{(2)}$ and so is ϕ^*. The contact contribution of the integral over $\Gamma^{(1)}$ is

$$G(\varphi_t, \varphi^*) + G_c(\varphi_t, \varphi^*) = 0, \qquad G_c(\varphi_t, \varphi^*) = -\int_{\Gamma^{(1)}} t_t^{(1)}(X) \cdot \{\varphi^{*(1)}(X) - \varphi^{*(2)}[\overline{Y}(X)]\}d\Gamma^{(1)}.$$

The statement of the contact virtual work is given by

$$G_c(\varphi_t, \varphi^*) = -\int_{\Gamma^{(1)}} [t_N v - t_{T_\alpha} \tau^\alpha] \cdot [\varphi^{*(1)}(X) - \varphi^{*(2)}(\overline{Y}(X))]d\Gamma^{(1)} = \int_{\Gamma^{(1)}} [t_{N_t} \delta g - t_{T\alpha_t} \delta \xi_-^\alpha]d\Gamma^{(1)}.$$

3. Numerical solution

3.1. *Penalty regularization of constraints.*
The solution of boundary problems subject to restrictions such as those presented in Equation (2) for normal contact and in Equation (4) for the Coulomb friction laws is carried out here with a penalty formulation by which the restrictions are approximated through an easy-to-implement procedure. For normal contact, a normal penalty parameter ε_N is introduced in the definition of the constitutive relation of the normal force $t_N = \varepsilon_N \langle g \rangle$, where $\langle \cdot \rangle$ denotes the positive part of the operand.

By introducing a tangential penalty ε_T, the regularization for the frictional response is expressed as

$$\mathbf{\Phi} := \|t_T^b\| - \mu t_N \leq 0, \qquad v_T^b - \zeta \frac{t_T^b}{\|t_T^b\|} = \frac{1}{\varepsilon_T} L_v t_T^b, \qquad \zeta \geq 0, \qquad \mathbf{\Phi}\zeta = 0,$$

where $L_v t_T^b := \dot{t}_{T_\alpha} t^\alpha$ is the Lie derivative of the tangential force. The above regularization is exact only in the limit $\varepsilon_N \to \infty$ and $\varepsilon_T \to \infty$, in which case the slip rate $\zeta t_T^b / \|t_T^b\|$ equals the relative velocity v_T^b. These relations are easy to incorporate in the virtual work principle and subsequently implement in a finite element procedure. For frictional problems, the tangential gap function is introduced as $g_T^\alpha = \overline{\xi_{n+1}^\alpha} - \overline{\xi_n^\alpha}$.

3.2. *Incremental finite element formulation.*
The boundary value problem can be solved incrementally by considering a set of subintervals $U_{n=0}^N [t_n, t_{n+1}]$. The evolution equations for the constitutive model are obtained through numerical integration. Here we adopt an implicit Euler algorithm. In the framework

of a consistent linearization, the contact virtual work is defined according to

$$\Delta G^c(\varphi_t, \varphi^*) = \Delta \left\{ \int_{\Gamma_c^{(1)}} \left[t_N \delta g + t_{T_\alpha} \cdot \delta \overline{\xi^\alpha} \right] d\Gamma \right\} = \int_{\Gamma_c^{(1)}} \left[\Delta(t_N \delta g) + \Delta t_{T_\alpha} \delta \overline{\xi^\alpha} + t_{T_\alpha} \Delta \delta \overline{\xi^\alpha} \right] d\Gamma^{(1)}, \quad (5)$$

where t_N are contact pressures and t_T frictional tractions. The quantity $\Delta(\delta g)$ is computed by linearizing δg, which is the linearized variation of the gap function, $\delta \overline{\xi}$ is obtained by application of the orthogonality condition of the tangent vectors with the normal vector, and $\Delta(\delta \overline{\xi})$ is obtained by computing the directional derivative of the orthogonality condition.

For finite element discretization of the domain, the contact virtual work expression in discrete form is

$$G_c(\varphi_t^h, \varphi^{*h}) = \int_{\Gamma^{(i)h}} \left[t_{Nt}^h \delta g^h + t_T^h \delta \overline{\xi^{\alpha h}} \right] d\Gamma^{(1)^h},$$

where the discrete counterparts of $\phi^{(i)}$ and $\phi^{*(i)}$ are $\phi^{(i)^h}$ and $\phi^{*(i)^h}$, defined over individual element surfaces as $\phi_e^{(i)^h}(\eta) = \Sigma N^a(\eta)\phi_a^{(i)}$ for $a = 1, \ldots, n_e$. The term $\phi_a^{(i)}$ is the nodal value of $\phi^{(i)^h}$, n_e is the number of nodes per element surface, $N^a(\eta)$ is an isoparametric shape function for three-dimensional problems. Using the same scheme $X_e^h(\eta) = \Sigma N^a(\eta)X_a$.

Solution of the weak form of equilibrium is obtained here with the Newton–Raphson method, which requires linearization of Equation (5). For numerical integration, the linearized virtual contact work is

$$\Delta G_c(\varphi^h, \varphi^{*h}) \approx \sum_{j=1}^{n_{\rm el}} \sum_{k=1}^{n_{\rm int}} W^k j(\eta^k) \left[\Delta \left[t_N^h(\eta^k) \delta g^h(\eta^k) \right] + \Delta t_{T_\alpha}^h(\eta^k) \delta \overline{\xi^{\alpha h}}(\eta^k) + t_{T_\alpha}^h(\eta^k) \Delta \left[\delta \overline{\xi^{\alpha h}}(\eta^k) \right] \right],$$

where $n_{\rm int}$ is the number of integration points on each contact surface element $\Gamma^{(1)^h}$, W^k is the integration weight factor, $\delta \Phi_c^k$ is the vector of nodal displacement variations, R_c^k is the residual vector, and the index k indicates the number of the integration point. The terms $\delta g^h(\eta^k)$ are the variations of g and the simplification of the variation $\delta \overline{\xi^{\alpha h}}(\eta^k)$ with the corresponding discrete fields. Expression (5) can now be written as

$$\Delta G_c(\varphi^h, \varphi^{*h}) = \sum_{j=1}^{n_{\rm el}} \sum_{k=1}^{n_{\rm int}} W^k j(\eta^k) \delta \Phi_c^k \cdot K_c^k \Delta \Phi_c^k. \quad (6)$$

In the above equation K_c^k is the contact stiffness matrix. The linearized contact terms $\Delta \left[t_N^h(\eta^k) \delta g^h(\eta^k) \right]$ and $\Delta \left[\delta \overline{\xi^{\alpha h}}(\eta^k) \right]$ are given by their corresponding discrete components. Vector $\Delta \Phi_c^k$ contains the nodal displacement values u^h, which take part at contact. The term $\Delta t_T^h(\eta^k)$ is obtained by a classical plasticity return algorithm. In the present work a nodal quadrature is employed by the evaluation of Equation (6) as presented in detail in [Ferreira and Roehl 2001].

The finite element discretization is carried out with eight-node hybrid brick elements based on an enhanced assumed strain formulation in the framework of large strain J2 plasticity; for details see [Simo et al. 1985; Roehl and Ramm 1996]. In this case the node-to-surface contact involves five nodes as illustrated in Figure 4.
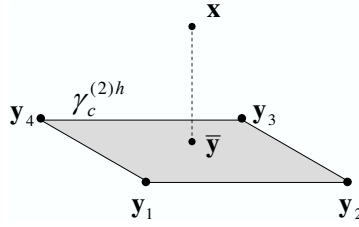
Figure 4. Slave node and master surface.

Accordingly, $\delta\Phi$ contains the displacement variations of the contacting slave node $\varphi^{*(1)}(X)$ and those of the four nodes on finite element on the master surface $\gamma_e^{(2)^h}(\varphi^{*(2)}(Y))$:

$$\delta\Phi = \begin{bmatrix} \varphi^{*(1)}(X) \\ \varphi^{*(2)}(Y_1) \\ \varphi^{*(2)}(Y_2) \\ \varphi^{*(2)}(Y_3) \\ \varphi^{*(2)}(Y_4) \end{bmatrix}, \qquad \Delta\Phi = \begin{bmatrix} u^{(1)}(X) \\ u^{(2)}(Y_1) \\ u^{(2)}(Y_2) \\ u^{(2)}(Y_3) \\ u^{(2)}(Y_4) \end{bmatrix}.$$

4. Applications

4.1. *Benchmark for soil-structure interface contact.* Figure 5 (left) illustrates a long elastic block (that is, $L \gg H$) loaded in compression at one end and restrained at the other. The block is also restrained against compression in the x direction by the frictional contact model along its base. No strain is permitted in either the y or z direction. The block has length $L = 10\,\mathrm{m}$ with $L/H = 10$, Young's modulus $E = 1.0 \times 10^5$ kPa, Poisson's coefficient $v = 0.0$, and the initial value of applied stress $P = 100$ kPa.

For this analysis the penalty method was used with normal and tangential penalties equal to $\varepsilon_N = 10^4$ and $\varepsilon_T = 10^8$, respectively. The Coulomb frictional law at the block-foundation interface has friction coefficient $\mu = 0.5$. The analysis was executed under loading control conditions. The system was modeled by a finite element mesh consisting of 20 eight-node hexahedral elements; see Figure 5 (right). The results for the horizontal displacements at the contact interface obtained in this analysis were compared with the results obtained in the numerical solutions developed for [Hird and Russell 1990] for different load levels as shown in Figure 6.

4.2. *Buried pipeline.* Figure 7 shows a buried steel pipe of diameter $D_0 = 1$ m embedded at a depth $2D_0$ with the following mechanical and geometrical properties: axial stiffness $EA = 4.2 \times 10^5$ kN, flexural
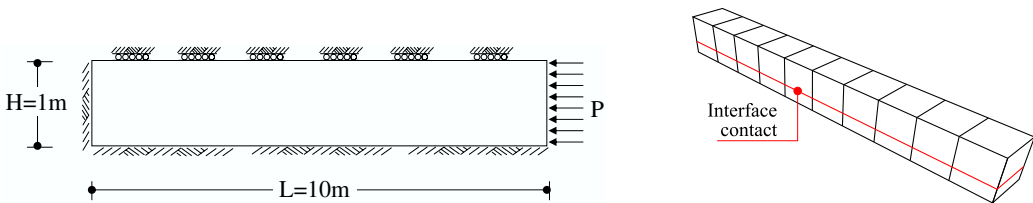

Figure 5. Definition of the long elastic block problem (left). Finite element mesh (right).
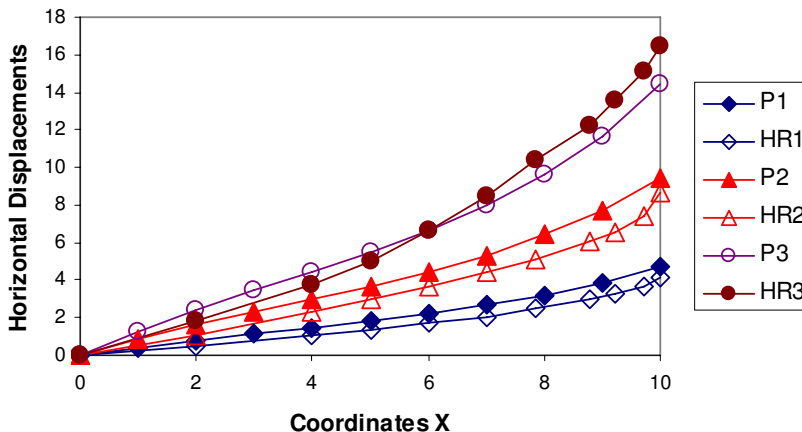
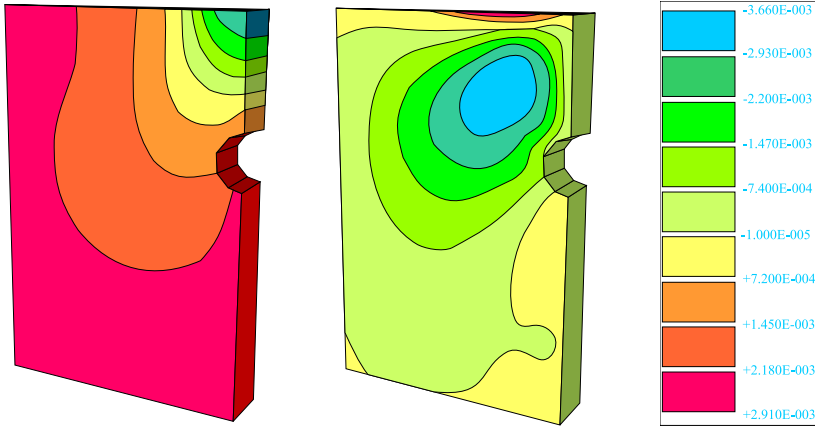**Figure 6.** Horizontal displacements at contact interface; results of CARAT versus [Hird and Russell 1990].

stiffness $EI = 0.1\,\text{kN·m}^2$, thickness $t = 2\,\text{mm}$, and Poisson's ratio $\nu_p = 0.3$. The linear elastic soil layer has thickness $H = 8\,\text{m}$, Young's modulus $E = 2.7 \times 10^3\,\text{kPa}$, and Poisson's ratio $\nu_s = 0.33$. The soil layer is submitted to a strip load $q = 100\,\text{kPa}$, uniformly distributed over a length $B = 2\,\text{m}$ in the xy-plane; see Figure 6.

Due to symmetry, only half of the soil-pipe system was modeled by a finite element mesh (Figure 7, right), consisting of 365 eight-node elements (brick8). The analysis was carried out under the assumption of plane strain conditions, by preventing axial displacements through the introduction of proper boundary constraints. The frictional coefficient was considered to be $\mu = 0.5$, and the penalty parameters were $\varepsilon_N = 10^4$ and $\varepsilon_T = 10^8$. The analysis was executed under displacement control conditions. Figure 8 shows the horizontal and vertical field displacement of the soil-pipe system according to the frictional contact formulation.
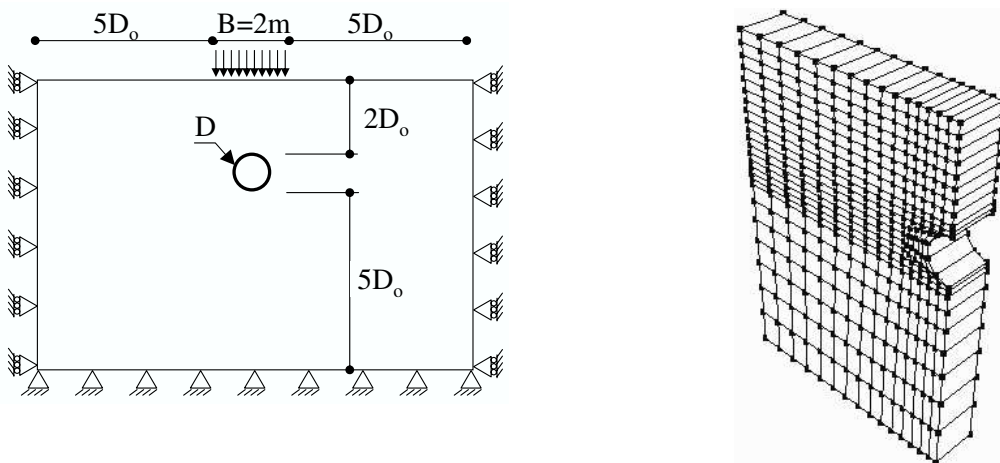
Figure 7. Geometry of the soil-pipe system (left). Finite element mesh (right).

Figure 8. Vertical (left) and horizontal (right) displacement fields according to the frictional contact formulation.

4.3. *Soil-pipe interaction: three-dimensional model.* In this example the elastic behavior of the soil is considered with Young's modulus $E = 50.0$ MPa and Poisson's coefficient $v = 0.2$. The pipeline assumes an elasto-plastic constitutive model based on the von Mises criteria with isotropic hardening. The yielding stress and the tangent modulus are $S_y = 420$ MPa and $E_T = 75000$ MPa, respectively. Pipe properties are listed in Table 1.

The loading applied to the pipeline consists in an internal pressure equal to 9.0 MPa, transversal load of 1000.0 N/m, and the overburden ($\gamma = 1.8$ KN/m^3), according to Table 2.

Due to symmetry, only half of the soil-pipe system is modeled by a finite element mesh (longitudinal direction), consisting of 622 eight-node hybrid brick elements (Hexa8-E3). Pipeline geometry and the finite element model are shown in Figure 9. The frictional coefficient is considered to be $\mu = 0.1$ and the penalty parameters are $\varepsilon_N = 10^2$ and $\varepsilon_T = 10^2$. The analysis was carried out under load control conditions. The frictional contact problem formulation simulates the soil-pipe interface behavior.

The internal pressure induces longitudinal stresses in the pipe due to Poisson's effect; see Figure 10. These longitudinal stresses arise when the pipe is restricted at its ends and/or by the presence of longitudinal friction. We have verified that the pipe has achieved yielding; see Figure 10.

Parameter	Value
I_{zz} (m^4)	7.9516531×10^{-5}
A (m^2)	6.2586416×10^{-3}
De (m)	0.325
Di (m)	0.3125
t (m)	0.00625

Table 1. Pipe properties.

Distance	Overburden	Additional Load	Internal Pressure
0 – 5.0 m	X	X	X
5.0 – 6.5 m	X	-	X
6.5 – 8.0 m	-	-	X
8.0 – 13.0 m	-	-	X

Table 2. Pipeline load.
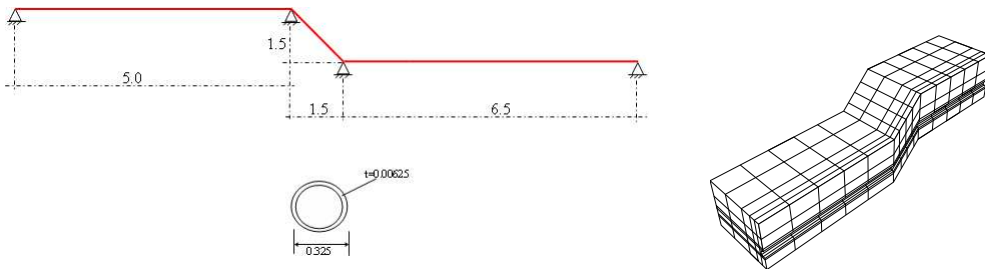
Figure 9. The pipeline geometry in the yz-plane (left). Finite element mesh: 622 Hexa8-EAS elements (right).
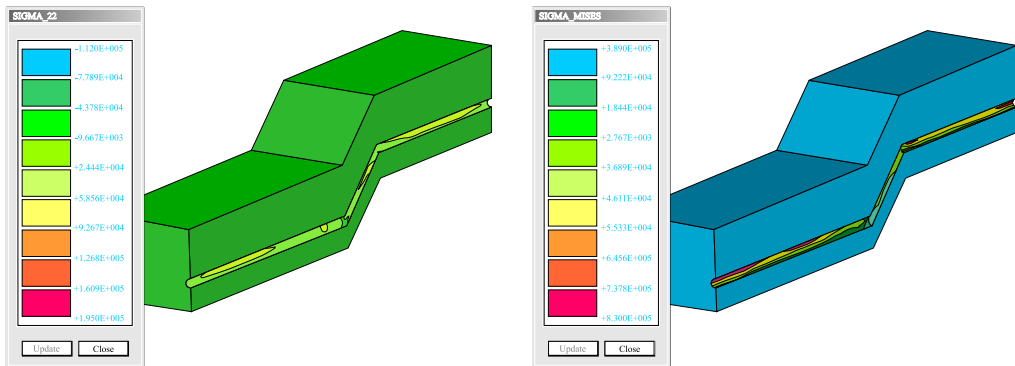
Figure 10. Longitudinal stresses and von Mises stresses obtained with our model.

5. Conclusion

This work presents a finite element numerical model for the analysis of buried pipes. The solution of elasto-plastic contact problem includes the presence of large elasto-plastic strains. The contact conditions are imposed through a penalty formulation that has been proven quite effective in the cases studied, if the penalty parameters are adequately chosen. For problems in which the contacting bodies present stiffness of the same order of magnitude the choice of these parameters is not difficult. Large normal contact forces make the parameter calibration more troublesome.

This is not usually the case by pipe-soil systems. An application of the model to the problem of a buried pipe under close to site conditions illustrates the effectiveness of the soil-pipe interaction model for more realistic engineering problems.

References

[Bathe and Chaudhary 1985] K. J. Bathe and A. Chaudhary, "A solution method for planar and axisymmetric contact problems", *Int. J. Numer. Methods Eng.* **21** (1985), 65–88.

[Desai et al. 1984] C. S. Desai et al., "Thin-layer element for interfaces and joints", *Int. J. Numer. Anal. Methods Geomech.* **8** (1984), 19–43.

[Ferreira and Roehl 2001] K. I. Ferreira and D. Roehl, "Three dimensional elastoplastic contact analysis at large strains with enhanced assumed strain elements", *Int. J. Solids Struct.* **38** (2001), 1855–1870.

[Hird and Russell 1990] C. Hird and D. Russell, "A benchmark for soil-structure interface elements", *Comput. Geotech.* **10** (1990), 139–147.

[Katona 1983] M. Katona, "A simple contact-friction interface element with applications to buried culverts", *Int. J. Numer. Anal. Methods Geomech.* **7** (1983), 371–384.

[Kwak and Lee 1988] B. M. Kwak and S. S. A. Lee, "Complementarity problem formulation for two-dimensional frictional contact problems", *Comput. Struct.* **28** (1988), 469–480.

[Laursen 2002] T. A. Laursen, *Computational contact and impact mechanics*, Springer-Verlag, Berlin, 2002. Fundamentals of modeling interfacial phenomena in nonlinear finite element analysis. MR 1902698 (2003e:74050)

[Laursen and Simo 1993] T. A. Laursen and J. C. Simo, "A continuum-based finite element formulation for the implicit solution of multibody, large deformation frictional contact problems", *Int. J. Numer. Methods Eng.* **36** (1993), 3451–3485.

[Lee et al. 1994] S. C. Lee, B. M. Kwak, and O. K. Kwon, "Analysis of incipient sliding contact by three-dimensional linear complementarity problem formulation", *Comput. Struct.* **53** (1994), 695–708.

[Lim et al. 2001] M. L. Lim, M. K. Kim, T. W. Kim, and J. W. Jang, "The behavior analysis of buried pipeline considering longitudinal permanent ground deformation", in *Pipeline 2001: Advances in Pipelines Engineering & Construction* (San Diego, California), vol. 3, edited by J. P. Castronovo, 107, ASCE, 2001.

[Mandolini et al. 2001] Mandolini et al., "Coupling of underground pipelines and slowly moving landslides by bem analysis", *Comput. Model. Eng. Sci. CMES* **2**:1 (2001), 39–48.

[Peric and Owen 1992] D. Peric and R. J. Owen, "Computational model for 3D contact problems with friction based on the penalty method", *Int. J. Numer. Methods Eng.* **35** (1992), 1289–1309.

[Roehl and Ramm 1996] D. Roehl and E. Ramm, "Large elasto-plastic finite element analysis of solids and shells with the enhanced assumed strain concept", *Int. J. Solids Struct.* **33**:20–22 (1996), 3215–3237.

[Rubio et al. 2003] N. Rubio, D. Roehl, and C. Romanel, "Design of buried pipes considering the reciprocal soil-structure interaction", pp. 1279–1287 in *Pipelines 2003: New Pipeline Technologies, Security* (Baltimore, MD), edited by M. Najafi, ASCE, 2003.

[Selvadurai and Pang 1988] A. P. S. Selvadurai and S. Pang, "Non-linear effects in soil-pipeline interaction in the ground subsidence zone", pp. 1085–1094 in *Proc. 6th Intr. Conf. Numer. Methods in Geomechanics* (Innsbruck), vol. 2, A. A. Balkema, 1988.

[Simo et al. 1985] J. C. Simo, P. Wriggers, and R. L. Taylor, "A perturbed Lagrangian formulation for the finite element solution of contact problems", *Comput. Methods Appl. Mech. Eng.* **50** (1985), 163–180.

[Zhou and Murray 1993] Z. Zhou and D. Murray, *Behavior of buried pipelines subjected to imposed deformations*, vol. Volume V, Pipeline Technology, ASME, 1993. OMAE.

[Zhou and Murray 1996] Z. Zhou and D. Murray, "Pipeline beam models using stiffness property deformation relations", *J. Transp. Eng.* **122**:2 (1996), 164–172.

NELLY PIEDAD RUBIO: nrubio@civ.puc-rio.br
Civil Engineering Department, Pontifícia Universidade Católica do Rio de Janeiro, CEP 22453-900 Rio de Janeiro, Brazil

DEANE ROEHL: droehl@civ.puc-rio.br
Civil Engineering Department, Pontifícia Universidade Católica do Rio de Janeiro, CEP 22453-900 Rio de Janeiro, Brazil

CELSO ROMANEL: romanel@civ.puc-rio.br
Civil Engineering Department, Pontifícia Universidade Católica do Rio de Janeiro, CEP 22453-900 Rio de Janeiro, Brazil